2014 IEEE International Conference on Robotics & Automation (ICRA)
Hong Kong Convention and Exhibition Center
May 31 - June 7, 2014. Hong Kong, China

Finite-gain L_2 Stability of Anti-windup Adaptive Tracking Control for Euler-Lagrange Systems with Actuator Saturation

Mitsuru Kanamori

***Abstract*-The present paper describes finite-gain L_2 stability guaranteed locally by the proposed anti-windup adaptive law for Euler–Lagrange systems with actuator saturation. All constant parameters of the robot system are estimated for an arbitrary target orbit. In order to achieve finite-gain L_2 stability and ensure adaptive tracking performance, an output saturation function of the tracking error is introduced. The finite L_2 gains are derived considering four actuator saturation cases, and finite-gain L_2 stability is guaranteed locally based on passivity. The control performance is verified through numerical simulations using a two-link robot arm.**

I. Introduction

All plant systems consist of input limitations, so that the systems are protected from damage caused by over input or to limit actuator performance. Input restriction increases the windup phenomenon, which causes undesirable degradation of the control performance. Over the past decade, considerable research has been carried out on stabilization and controller design for linear systems with actuator saturation. However, a few studies have investigated adaptive tracking control considering input saturation for nonlinear Euler–Lagrange systems, even though robot systems are expected to achieve tracking control performance [1]-[5]. An adaptive proportional and derivative controller design method for robot manipulators was presented, and the asymptotic stability was described by Arimoto based on the concept of quasi-natural potential [6]. Based on passivity, an anti-windup adaptive tracking control method for non-linear Euler–Lagrange systems has been proposed by Kanamori [7]. In this method, although global asymptotic stability has been guaranteed, the input output stability or robustness has not been discussed. It is well known that passivity is applicable to finite-gain L_2 stability [8], and the method proposed by Kanamori [7] is expected to extend to finite-gain L_2 stability. In the present paper, finite-gain L_2 stability is described for the anti-windup adaptive tracking control proposed by Kanamori for nonlinear Euler–Lagrange systems with actuator saturation. Some properties for finite-gain L_2 stability are listed. Using the proposed anti-windup adaptive law, all constant parameters of the robot system are estimated for an arbitrary target orbit, and based on the concept of quasi-natural potential, the output saturation function for the tracking error is introduced [6]. The finite L_2 gains are derived considering four actuator saturation cases, and finite-gain L_2 stability is guaranteed locally based on passivity. The control performance of the proposed controller is demonstrated through numerical simulations using a two-link robot arm.

Manuscript received January 17, 2013. M. Kanamori is with the Maizuru National College of Technology, Maizuru, Kyoto 625-8511, Japan (Phone: +81-773-62-8955; Fax: +81-773-62-8955; E-mail: kanamori@maizuru-ct.ac.jp).

II. Preliminaries

Consider a class of dissipative Euler–Lagrange robot systems represented as

$$\boldsymbol{H}(\boldsymbol{q})\ddot{\boldsymbol{q}} + \{\boldsymbol{B}_0 + \frac{1}{2}\dot{\boldsymbol{H}}(\boldsymbol{q}) + \boldsymbol{S}(\boldsymbol{q},\dot{\boldsymbol{q}})\}\dot{\boldsymbol{q}} + \boldsymbol{g}(\boldsymbol{q}) = \sigma(\boldsymbol{u}+\boldsymbol{d}_1) + \boldsymbol{d}_2 , \tag{1}$$

where $\boldsymbol{q} = [q_1 \ \ .... \ \ q_n]^T$ represents the angular vector of each joint, $\boldsymbol{H}(\boldsymbol{q}) \in \boldsymbol{R}^{n\times n}$ is the positive definite inertia matrix, $\boldsymbol{B_0} \in \boldsymbol{R}^{n\times n}$ is the positive diagonal constant matrix derived from the Raleigh dissipation function, $\boldsymbol{S}(\boldsymbol{q},\dot{\boldsymbol{q}}) \in \boldsymbol{R}^{n\times n}$ is the skew-symmetric matrix, and $\boldsymbol{g}(\boldsymbol{q})$ is the gravity term. Here, $\boldsymbol{u} = [u_1 \ \ .... \ \ u_n]^T$ is the control input torque vector, and $\boldsymbol{\sigma}(\boldsymbol{u}) = [\sigma(u_1) \ \ ..... \ \ \sigma(u_n)]^T$ is the saturated input torque vector, which is defined as follows:

$$\begin{aligned} &\text{if } u_{i\min} \le u_i \le u_{i\max} ,\ \sigma(u_i) = u_i , \\ &\text{if } 0 < u_{i\max} < u_i , \quad \sigma(u_i) = u_{i\max} , \\ &\text{if } u_i < u_{i\min} < 0 , \quad \sigma(u_i) = u_{i\min} , \end{aligned} \tag{2}$$

where $|u_{i\max}| = |u_{i\min}|$ for $i = 1,...., n$. $\boldsymbol{d}_i = [d_{i1} \ \ .... \ \ d_{in}]^T$ is a disturbance that belongs to L_2 for $i = 1, 2$. The augmented disturbance $\boldsymbol{d}$ is represented as

$$\boldsymbol{d} = [\boldsymbol{d}_1^T \ \ \boldsymbol{d}_2^T]^T , \ \int_0^\infty \boldsymbol{d}^T\boldsymbol{d}dt < \infty . \tag{3}$$

The estimation function of control input saturation, $\psi(\boldsymbol{u}) = [\psi(u_1) \ \ ... \ \ \psi(u_n)]^T$ is introduced as

$$\psi(\boldsymbol{u}) = \boldsymbol{u} - \sigma(\boldsymbol{u}) , \tag{4}$$

where

$$\begin{aligned} &\text{if } u_{i\min} \le u_i \le u_{i\max} ,\ \psi(u_i) = 0 , \\ &\text{if } 0 < u_{i\max} < u_i , \quad \psi(u_i) = u_i - u_{i\max} > 0 , \\ &\text{if } u_i < u_{i\min} < 0 , \quad \psi(u_i) = u_i - u_{i\min} < 0 . \end{aligned} \tag{5}$$

The asymptotic control input, denoted by $\boldsymbol{u}_d$, that makes the tracking error zero is given in the following form, with the target vector denoted by $\boldsymbol{q}_d$:

$$\boldsymbol{H}(\boldsymbol{q}_d)\ddot{\boldsymbol{q}}_d+\{\boldsymbol{B}_0+\frac{1}{2}\dot{\boldsymbol{H}}(\boldsymbol{q}_d)+\boldsymbol{S}(\boldsymbol{q}_d,\dot{\boldsymbol{q}}_d)\}\dot{\boldsymbol{q}}_d+\boldsymbol{g}(\boldsymbol{q}_d)=\boldsymbol{u}_d\,. \tag{6}$$

The tracking error denoted by $\Delta\boldsymbol{q}$ is given by

$$\Delta\boldsymbol{q}=\boldsymbol{q}-\boldsymbol{q}_d\,. \tag{7}$$

In order to achieve tracking control for any target orbit, the following assumption is introduced:
Assumption 1: *Asymptotic control input* $\boldsymbol{u}_d$*, as shown in (6), remains in the possible input range*

$$u_{i\min}<u_{di}<u_{i\max}\,,\ i=1,....,n\,. \tag{8}$$

For the disturbance entered into the input saturation function, the following property is introduced.
Property 1: *The saturated control input with disturbance* $\boldsymbol{d}_1$*, namely* $\boldsymbol{\sigma}(\boldsymbol{u}+\boldsymbol{d}_1)$*, may be represented as*

$$\boldsymbol{\sigma}(\boldsymbol{u}+\boldsymbol{d}_1)=\boldsymbol{\sigma}(\boldsymbol{u})+\delta\boldsymbol{\psi}(\boldsymbol{u},\boldsymbol{d}_1)\,, \tag{9}$$

where

$$\delta\boldsymbol{\psi}(\boldsymbol{u},\boldsymbol{d}_1)=\boldsymbol{\psi}(\boldsymbol{u})-\boldsymbol{\psi}(\boldsymbol{u}+\boldsymbol{d}_1)+\boldsymbol{d}_1\,. \tag{10}$$

Then, the following relation holds:

$$\delta\boldsymbol{\psi}(\boldsymbol{u},\boldsymbol{d}_1)^T\,\delta\boldsymbol{\psi}(\boldsymbol{u},\boldsymbol{d}_1)\le\boldsymbol{d}_1{}^T\boldsymbol{d}_1\,. \tag{11}$$

Outline Proof of Property 1: *See Proof of Property 1 on page 2 in Reference [8].*
Subtracting (6) from (1), the closed-loop system may be represented as

$$\boldsymbol{F}(\boldsymbol{q},\dot{\boldsymbol{q}},\Delta\dot{\boldsymbol{q}},\Delta\ddot{\boldsymbol{q}},\boldsymbol{h})+\boldsymbol{J}(\boldsymbol{\sigma}(\boldsymbol{u}),\boldsymbol{u}_d)=\delta\boldsymbol{\psi}(\boldsymbol{u},\boldsymbol{d}_1)+\boldsymbol{d}_2\,. \tag{12}$$

The first function of the left-hand side of (12) captures the robot dynamics in the given system and is represented as

$$\begin{aligned}\boldsymbol{F}(\boldsymbol{q},\dot{\boldsymbol{q}},\Delta\dot{\boldsymbol{q}},\Delta\ddot{\boldsymbol{q}};\boldsymbol{h})=&\ \boldsymbol{H}(\boldsymbol{q})\Delta\ddot{\boldsymbol{q}}+\{\boldsymbol{B}_0+\frac{1}{2}\dot{\boldsymbol{H}}(\boldsymbol{q})+\boldsymbol{S}(\boldsymbol{q},\dot{\boldsymbol{q}})\}\Delta\dot{\boldsymbol{q}}\\&+\boldsymbol{h}(\Delta\boldsymbol{q},\Delta\dot{\boldsymbol{q}})\,,\end{aligned} \tag{13}$$

where

$$\begin{aligned}\boldsymbol{h}(\Delta\boldsymbol{q},\Delta\dot{\boldsymbol{q}})=&\ \{\boldsymbol{H}(\boldsymbol{q})-\boldsymbol{H}(\boldsymbol{q}_d)\}\ddot{\boldsymbol{q}}_d\\&+\{\frac{1}{2}\dot{\boldsymbol{H}}(\boldsymbol{q})-\frac{1}{2}\dot{\boldsymbol{H}}(\boldsymbol{q}_d)+\boldsymbol{S}(\boldsymbol{q},\dot{\boldsymbol{q}})-\boldsymbol{S}(\boldsymbol{q}_d,\dot{\boldsymbol{q}}_d)\}\dot{\boldsymbol{q}}_d\\&+\{\boldsymbol{g}(\boldsymbol{q})-\boldsymbol{g}(\boldsymbol{q}_d)\}\,.\end{aligned} \tag{14}$$

The second function of the left-hand side of (12) concerns the controller and the asymptotic control input represented as

$$\boldsymbol{J}(\boldsymbol{\sigma}(\boldsymbol{u}),\boldsymbol{u}_d)=-\boldsymbol{\sigma}(\boldsymbol{u})+\boldsymbol{u}_d\,. \tag{15}$$

The right-hand side of (12) is the disturbance input. Let us choose the following $\boldsymbol{y}$ for the output, as shown in Arimoto [6]:

$$\boldsymbol{y}=\Delta\dot{\boldsymbol{q}}+\alpha\boldsymbol{s}(\Delta\boldsymbol{q})\,. \tag{16}$$

The symbol α is an appropriate positive real number. The function $\boldsymbol{s}(\Delta\boldsymbol{q})$ is an output saturation function described as follows:

$$\boldsymbol{s}(\Delta\boldsymbol{q})=\begin{bmatrix}s_1(\Delta q_1) & s_2(\Delta q_2) & \ldots\ldots & s_n(\Delta q_n)\end{bmatrix}^T\,, \tag{17}$$

where $s_i(x_i)$ is the Lipschitz function depicted in Fig. 1(a).
Property 2: *For the output saturation function shown in (17), the following properties are ensured.*
(a) There exists a positive convex function $S_i(x_i)$*, as shown in Fig. 1(b), such that the following relation is satisfied:*

$$\frac{dS_i(x_i)}{dx_i}=s_i(x_i)\,. \tag{18}$$

Then, the following relations hold:

$$\dot{S}_i(\Delta q_i)=s_i(\Delta q_i)\Delta\dot{q}_i\,,\ \sum_i\dot{S}_i(\Delta q_i)=\boldsymbol{s}(\Delta\boldsymbol{q})^T\dot{\boldsymbol{q}}\,. \tag{19}$$

(b) There exist positive real constants c_i *and* c_{0i} *such that the following inequalities are satisfied:*

$$S_i(\Delta q_i)\ge c_i s_i(\Delta q_i)^2\,, \tag{20}$$

$$\begin{aligned}\min\{&|u_{i\max}-u_{di}|,|u_{i\min}-u_{di}|\}\\&\ge c_{0i}|s_i(\Delta q_i)|_{\max}\ge c_{0i}|s_i(\Delta q_i)|\,.\end{aligned} \tag{21}$$

For the passivity and L_2 stability, the inner product between the closed-loop system (12) and the output $\boldsymbol{y}$, as shown in (16), is required. Thus, the following properties are introduced.

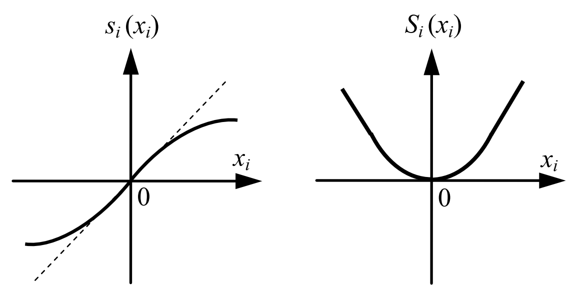

(a) Function $s_i(x_i)$ (b) Function $S_i(x_i)$

Figure 1. Output saturation function $s_i(x_i)$ and convex function $S_i(x_i)$.

Property 3: *For the inner product of the input disturbances in (12) and the output* $\boldsymbol{y}$*, the following inequality holds:*

$$\boldsymbol{y}^T\{\delta\boldsymbol{\psi}(\boldsymbol{u},\boldsymbol{d}_1)+\boldsymbol{d}_2\}$$
$$\le \frac{1}{\rho}\Delta\dot{\boldsymbol{q}}^T\Delta\dot{\boldsymbol{q}}+\frac{1}{\eta}\alpha\boldsymbol{s}(\Delta\boldsymbol{q})^T\boldsymbol{s}(\Delta\boldsymbol{q})+\frac{1}{2}(\rho+\alpha\eta)\boldsymbol{d}^T\boldsymbol{d}\,. \tag{22}$$

Outline proof of Property 3: *Using the following relations:*

$$\frac{1}{2}\left(\frac{1}{\sqrt{\rho}}\Delta\dot{\boldsymbol{q}}-\sqrt{\rho}\delta\boldsymbol{\psi}(\boldsymbol{u},\boldsymbol{d}_1)\right)^T\left(\frac{1}{\sqrt{\rho}}\Delta\dot{\boldsymbol{q}}-\sqrt{\rho}\delta\boldsymbol{\psi}(\boldsymbol{u},\boldsymbol{d}_1)\right)\ge 0\,, \tag{23}$$

$$\frac{1}{2}\left(\frac{1}{\sqrt{\rho}}\Delta\dot{\boldsymbol{q}}-\sqrt{\rho}\boldsymbol{d}_2\right)^T\left(\frac{1}{\sqrt{\rho}}\Delta\dot{\boldsymbol{q}}-\sqrt{\rho}\boldsymbol{d}_2\right)\ge 0\,, \tag{24}$$

$$\frac{\alpha}{2}\left(\frac{1}{\sqrt{\mu}}\boldsymbol{s}(\Delta\boldsymbol{q})-\sqrt{\mu}\delta\boldsymbol{\psi}(\boldsymbol{u},\boldsymbol{d}_1)\right)^T\left(\frac{1}{\sqrt{\mu}}\boldsymbol{s}(\Delta\boldsymbol{q})-\sqrt{\mu}\delta\boldsymbol{\psi}(\boldsymbol{u},\boldsymbol{d}_1)\right)\ge 0\,, \tag{25}$$

$$\frac{\alpha}{2}\left(\frac{1}{\sqrt{\mu}}\boldsymbol{s}(\Delta\boldsymbol{q})-\sqrt{\mu}\boldsymbol{d}_2\right)^T\left(\frac{1}{\sqrt{\mu}}\boldsymbol{s}(\Delta\boldsymbol{q})-\sqrt{\mu}\boldsymbol{d}_2\right)\ge 0\,, \tag{26}$$

as well as the first equation in (3) and the relation (11), the inequality of (22) is derived.

Property 4: *There exist positive real numbers* $\bar{c}_1$ *through* $\bar{c}_6$ *that depend only on* $\boldsymbol{q}_d, \dot{\boldsymbol{q}}_d$*, and* $\ddot{\boldsymbol{q}}_d$ *such that the following inequalities are satisfied:*

$$\boldsymbol{s}(\Delta\boldsymbol{q})^T\boldsymbol{h}(\Delta\boldsymbol{q},\Delta\dot{\boldsymbol{q}})\ge -\bar{c}_1\|\boldsymbol{s}(\Delta\boldsymbol{q})\|^2-\bar{c}_2\|\boldsymbol{s}(\Delta\boldsymbol{q})\|\cdot\|\Delta\dot{\boldsymbol{q}}\|, \tag{27}$$

$$\Delta\dot{\boldsymbol{q}}^T\boldsymbol{h}(\Delta\boldsymbol{q},\Delta\dot{\boldsymbol{q}})\ge -\bar{c}_3\|\boldsymbol{s}(\Delta\boldsymbol{q})\|\cdot\|\Delta\dot{\boldsymbol{q}}\|-\bar{c}_4\|\Delta\dot{\boldsymbol{q}}\|^2\,, \tag{28}$$

$$\boldsymbol{s}(\Delta\boldsymbol{q})^T\{-\frac{1}{2}\dot{\boldsymbol{H}}(\boldsymbol{q})+\boldsymbol{S}(\boldsymbol{q},\dot{\boldsymbol{q}})\}\Delta\dot{\boldsymbol{q}}-\dot{\boldsymbol{s}}(\Delta\boldsymbol{q})^T\boldsymbol{H}(\boldsymbol{q})\Delta\dot{\boldsymbol{q}}$$
$$\ge -\bar{c}_5\|\boldsymbol{s}(\Delta\boldsymbol{q})\|\cdot\|\Delta\dot{\boldsymbol{q}}\|-\bar{c}_6\|\Delta\dot{\boldsymbol{q}}\|^2\,. \tag{29}$$

In order to achieve adaptive tracking control, the following property is required.

Property 5*: The left-hand side of the Euler–Lagrange system (1) may be given in the following form such that the constant parameters are separated linearly from the variable matrix:*

$$\boldsymbol{H}(\boldsymbol{q})\ddot{\boldsymbol{q}}+\{\boldsymbol{B}_0+\frac{1}{2}\dot{\boldsymbol{H}}(\boldsymbol{q})+\boldsymbol{S}(\boldsymbol{q},\dot{\boldsymbol{q}})\}\dot{\boldsymbol{q}}+\boldsymbol{g}(\boldsymbol{q})=\boldsymbol{Y}(\boldsymbol{q},\dot{\boldsymbol{q}},\dot{\boldsymbol{q}},\ddot{\boldsymbol{q}})\boldsymbol{p}\,, \tag{30}$$

where $\boldsymbol{Y}(\boldsymbol{q},\dot{\boldsymbol{q}},\dot{\boldsymbol{q}},\ddot{\boldsymbol{q}})$ *is the variable function matrix excluding any constant parameter and* $\boldsymbol{p}$ *is a vector of the constant parameters of the given system. Using this notation, equation (6) may be represented as*

$$\boldsymbol{Y}(\boldsymbol{q}_d,\dot{\boldsymbol{q}}_d,\dot{\boldsymbol{q}}_d,\ddot{\boldsymbol{q}}_d)\boldsymbol{p}=\boldsymbol{u}_d\,. \tag{31}$$

For finite L_2 gain considering actuator saturation, the following properties are introduced.

Property 6*: For positive scalar constants* λ_1 *and* λ_2 *such that* $\lambda_1\le\lambda_2$ *and any vector variable* $\boldsymbol{x}(t)$ *which belongs to* L_2*, there exists a positive constant real number* $\bar{\lambda}$ *such that the following relation is satisfied:*

$$\lambda_1\int_0^{t1}\|\boldsymbol{x}(t)\|^2dt+\lambda_2\int_{t1}^{\infty}\|\boldsymbol{x}(t)\|^2dt=\bar{\lambda}\int_0^{\infty}\|\boldsymbol{x}\|^2dt\,, \tag{32}$$

where $\|\cdot\|$ *denotes the Euclidean norm of* $(\cdot)$*. Then, the following inequality holds:*

$$\lambda_1\le\bar{\lambda}\le\lambda_2\,. \tag{33}$$

Property 7: *For positive scalar constants* λ_i*,* $i=1,....,l$*, and any vector variable* $\boldsymbol{x}(t)=[x_1(t)\ \ ....\ \ x_n(t)]^T$ *which belongs to* L_2*, the following relations hold:*

$$\min\{\lambda_i\}\int_0^{\infty}\sum_{i=1}^{l}x_i^2(t)dt\le\int_0^{\infty}\sum_{i=1}^{l}\lambda_i x_i^2(t)dt\le\max\{\lambda_i\}\int_0^{\infty}\sum_{i=1}^{l}x_i^2(t)dt\,. \tag{34}$$

III. CONTROLLER DESIGN

In order to ensure that the equilibrium state achieves $(s(\Delta\boldsymbol{q}),\Delta\dot{\boldsymbol{q}},\boldsymbol{u})\to(0,0,\boldsymbol{u}_d)$ as $t\to\infty$, consider the following proportional and derivative control law with the estimated values of the asymptotic control input:

$$\boldsymbol{u}=-\boldsymbol{A}\Delta\boldsymbol{q}-\boldsymbol{B}\Delta\dot{\boldsymbol{q}}+\hat{\boldsymbol{u}}_d\,, \tag{35}$$

where $\boldsymbol{A}$ and $\boldsymbol{B}$ denote positive diagonal matrices, and $\hat{\boldsymbol{u}}_d$ is an estimated asymptotic input that is represented as follows:

$$\boldsymbol{Y}(\boldsymbol{q}_d,\dot{\boldsymbol{q}}_d,\dot{\boldsymbol{q}}_d,\ddot{\boldsymbol{q}}_d)\hat{\boldsymbol{p}}=\hat{\boldsymbol{u}}_d\,, \tag{36}$$

where $\hat{\boldsymbol{p}}$ is the estimated parameter vector. The parameter estimation error denoted by $\boldsymbol{\varepsilon}$ is represented as

$$\boldsymbol{\varepsilon}=\boldsymbol{p}-\hat{\boldsymbol{p}}\,. \tag{37}$$

Then, the control law given by (35) may be represented as

$$\boldsymbol{u}=-\boldsymbol{A}\Delta\boldsymbol{q}-\boldsymbol{B}\Delta\dot{\boldsymbol{q}}-\boldsymbol{Y}(\boldsymbol{q}_d,\dot{\boldsymbol{q}}_d,\dot{\boldsymbol{q}}_d,\ddot{\boldsymbol{q}}_d)\boldsymbol{\varepsilon}+\boldsymbol{u}_d\,. \tag{38}$$

For finite-gain L_2 stability, we have the following assumptions.

Assumption 2: *There exist positive real numbers* α *and* ξ *such that the following inequalities are satisfied:*

$$\min\{a_m, c_{0m}\}-\bar{c}_0>0\,, \tag{39}$$

$$b_{0m} - \max\left\{\frac{\alpha\gamma_M}{c_m}, \bar{b}_0\right\} > 0, \qquad (40)$$

where

$$\bar{c}_0 = \bar{c}_1 + \frac{1}{2\xi}(\bar{c}_2 + \bar{c}_5 + \frac{1}{\alpha}\bar{c}_3), \qquad (41)$$

$$\bar{b}_0 = \bar{c}_4 + \alpha\bar{c}_6 + \frac{\xi}{2}\{\alpha(\bar{c}_2 + \bar{c}_5) + \bar{c}_3\}, \qquad (42)$$

$$0 < \alpha \in R, \quad 0 < \xi \in R. \qquad (43)$$

The symbols c_m and c_{0m} denote the minimum values of c_i and c_{0i}, as shown in Property 2(b), for $i = 1,......,n$, respectively. The symbols a_m, b_{0m}, and b_m denote the minimum positive diagonal components of $\boldsymbol{A}$, $\boldsymbol{B}_0$, and $\boldsymbol{B}$, respectively, and γ_M is the maximum eigenvalue of $\boldsymbol{H}(\boldsymbol{q})$.

Let us consider the following four actuator saturation cases:

(I) $\Delta\dot{\boldsymbol{q}}^T\boldsymbol{\psi}(\boldsymbol{u}) \ge 0$ and $\boldsymbol{s}(\Delta\boldsymbol{q})^T\boldsymbol{\psi}(\boldsymbol{u}) \ge 0$,

(II) $\Delta\dot{\boldsymbol{q}}^T\boldsymbol{\psi}(\boldsymbol{u}) \ge 0$ *and* $\boldsymbol{s}(\Delta\boldsymbol{q})^T\boldsymbol{\psi}(\boldsymbol{u}) < 0$,

(III) $\Delta\dot{\boldsymbol{q}}^T\boldsymbol{\psi}(\boldsymbol{u}) < 0$ *and* $\boldsymbol{s}(\Delta\boldsymbol{q})^T\boldsymbol{\psi}(\boldsymbol{u}) \ge 0$,

(IV) $\Delta\dot{\boldsymbol{q}}^T\boldsymbol{\psi}(\boldsymbol{u}) < 0$ *and* $\boldsymbol{s}(\Delta\boldsymbol{q})^T\boldsymbol{\psi}(\boldsymbol{u}) < 0$.

Adopt the following anti-windup adaptive law according to the actuator saturation cases (I) through (IV):

$$\hat{\boldsymbol{p}} = -\boldsymbol{P}^{-1}\int_0^t \boldsymbol{Y}(\boldsymbol{q}_d, \dot{\boldsymbol{q}}_d, \dot{\boldsymbol{q}}_d, \ddot{\boldsymbol{q}}_d)^T\,\bar{\boldsymbol{y}}dt, \qquad (44)$$

$$\bar{\boldsymbol{y}} = \Delta\dot{\boldsymbol{q}} + \alpha\boldsymbol{s}(\Delta\boldsymbol{q}) \text{ for case (I)}, \qquad (45)$$

$$\bar{\boldsymbol{y}} = \Delta\dot{\boldsymbol{q}} \quad \text{for case (II)}, \qquad (46)$$

$$\bar{\boldsymbol{y}} = \alpha\boldsymbol{s}(\Delta\boldsymbol{q}) \quad \text{for case (III)}, \qquad (47)$$

$$\bar{\boldsymbol{y}} = 0 \quad \text{for case (IV)}, \qquad (48)$$

where $\boldsymbol{P}$ is a positive diagonal matrix. Taking the inner product of output $\boldsymbol{y}$, as shown in (16), and the closed-loop system (12), the following relation is derived:

$$\boldsymbol{y}^T\{\boldsymbol{F}(\boldsymbol{q}, \dot{\boldsymbol{q}}, \Delta\dot{\boldsymbol{q}}, \Delta\ddot{\boldsymbol{q}}, \boldsymbol{h}) + \boldsymbol{J}(\boldsymbol{\sigma}(\boldsymbol{u}), \boldsymbol{u}_d)\} \ge \frac{dV_\kappa}{dt} + W_\kappa, \qquad (49)$$

where

$$W_\kappa = \lambda_\kappa\|\Delta\dot{\boldsymbol{q}}\|^2 + \alpha\mu_\kappa\|\boldsymbol{s}(\Delta\boldsymbol{q})\|^2, \qquad (50)$$

and λ_κ and μ_κ are, respectively, constant scalar numbers that

TABLE I. VALUES OF κ, λ_κ, AND μ_κ

Case	κ	λ_κ	μ_κ
(I)	1	$b_{0m} + b_m - \bar{b}_0$	$a_m - \bar{c}_0$
(II)	2	$b_{0m} + b_m - \bar{b}_0$	$c_{0m} - \bar{c}_0$
(III)	3	$b_{0m} - \bar{b}_0$	$a_m - \bar{c}_0$
(IV)	4	$b_{0m} - \bar{b}_0$	$c_{0m} - \bar{c}_0$

are positive definite under the conditions in Assumption 2 and are switched according to saturation state, as shown in TABLE I. Here, V_κ is a positive definite function. The suffix κ is a natural number from 1 to 4, which corresponds to saturation cases (I) through (IV). The derivation of V_κ, W_κ, λ_κ, and μ_κ have been described in detail in Reference [7]. Taking the time integral of (49) with (12) and (50), the following relation is derived based on Property 6:

$$\int_0^\infty \boldsymbol{y}^T\{\delta\boldsymbol{\psi}(\boldsymbol{u}, \boldsymbol{d}_1) + \boldsymbol{d}_2\} \ge \bar{\lambda}\|\Delta\dot{q}\|_2^2 + \alpha\bar{\mu}\|\boldsymbol{s}(\Delta\boldsymbol{q})\|_2^2 - V(0), \qquad (51)$$

where $V(0)$ is the initial value of V_κ and $\|\cdot\|_2$ indicates the L_2 norm of $(\cdot)$ defined by

$$\|\cdot\|_2 = \left(\int_0^\infty \|\cdot\|^2 dt\right)^{1/2}. \qquad (52)$$

$\bar{\lambda}$ and $\bar{\mu}$ are positive scalar constants, based on Property 6, and satisfy

$$\lambda_m \le \bar{\lambda} \le \lambda_M, \quad \mu_m \le \bar{\mu} \le \mu_M, \qquad (53)$$

where the suffixes *m* and *M* denote, respectively, minimum and the maximum values. Based on Property 3 and relation (51), the following inequality is derived:

$$\|\boldsymbol{d}\|_2^2 + \frac{2V(0)}{\rho + \alpha\eta} \ge \frac{2(\rho\bar{\lambda} - 1)}{\rho(\rho + \alpha\eta)}\|\Delta\dot{\boldsymbol{q}}\|_2^2 + \frac{2\alpha(\eta\bar{\mu} - 1)}{\eta(\rho + \alpha\eta)}\|\boldsymbol{s}(\Delta\boldsymbol{q})\|_2^2. \qquad (54)$$

This implies that the dynamics is finite-gain L_2 stable if $\rho\bar{\lambda} > 1$ and $\eta\bar{\mu} > 1$. The above results are summarized as the following main theorem.

Main Theorem: *Assume that conditions (39) through (43) in Assumption 2 and the following conditions are satisfied:*

$$\rho > \frac{1}{\bar{\lambda}} \text{ and } \eta > \frac{1}{\bar{\mu}}. \qquad (55)$$

Adopt the anti-windup adaptive law shown in (44) through (48). Then, the system is finite-gain L_2 stable.

However, actuator saturation does not always occur in synchronization with the saturation case. When actuator saturation occurs independently on the other actuator, $\bar{\lambda}$ and $\bar{\mu}$ are, respectively, given by (53) based on Property 7. The function matrix $\boldsymbol{Y}(\boldsymbol{q}_d, \dot{\boldsymbol{q}}_d, \dot{\boldsymbol{q}}_d, \ddot{\boldsymbol{q}}_d)$ in (44) is generally non-diagonal, so that interference with each joint value of $\boldsymbol{y}$ arises. For the practical adaptive law, the following proposition is introduced.

Proposition (Practical anti-windup adaptive law): *For the adaptive PD control law shown in (35), the following anti-windup adaptive law guarantees finite-gain L_2 stability:*

$$\hat{\boldsymbol{p}} = -\boldsymbol{P}^{-1}\int_0^t \boldsymbol{Y}(\boldsymbol{q}_d, \dot{\boldsymbol{q}}_d, \dot{\boldsymbol{q}}_d, \ddot{\boldsymbol{q}}_d)^T(\bar{\boldsymbol{y}}_1 + \alpha\bar{\boldsymbol{y}}_2)dt, \tag{56}$$

$$\text{if } \Delta\dot{q}_i\psi(u_i) \geq 0, \text{ then } \bar{y}_{1i} = \Delta\dot{q}_i, \tag{57}$$

$$\text{if } \Delta\dot{q}_i\psi(u_i) < 0, \text{ then } \bar{y}_{1i} = 0, \tag{58}$$

$$\text{if } s_i(\Delta q_i)\psi(u_i) \geq 0, \text{ then } \bar{y}_{2i} = s_i(\Delta q_i), \tag{59}$$

$$\text{if } s_i(\Delta q_i)\psi(u_i) < 0, \text{ then } \bar{y}_{2i} = 0, \tag{60}$$

$$\text{for } i = 1, \ldots\ldots, n.,$$

where

$$\bar{\boldsymbol{y}}_k = [\bar{y}_{k1} \quad \ldots\bar{y}_{ki}\ldots \quad \bar{y}_{kn}]^T \text{ and } k = 1,2. \tag{61}$$

Remark 1: *V_4 in (49) is a Lyapunov function since V_4 corresponds to V_s in outline proof of the Main Theorem in Reference [7]. This implies that global asymptotic stability of the equilibrium state is guaranteed when disturbances $\boldsymbol{d}_1$ and $\boldsymbol{d}_2$ are zero.*

Remark 2*: From relation (54), the following inequalities are obtained:*

$$\|\boldsymbol{d}\|_2 \geq \gamma_1\|\Delta\dot{\boldsymbol{q}}\|_2 - \beta, \tag{62}$$

$$\|\boldsymbol{d}\|_2 \geq \gamma_2\|s(\Delta\boldsymbol{q})\|_2 - \beta. \tag{63}$$

The finite L_2 gains γ_1 and γ_2 become

$$\gamma_1 = \sqrt{\frac{2(\rho\bar{\lambda} - 1)}{\rho(\rho + \alpha\eta)}}, \ \gamma_2 = \sqrt{\frac{2\alpha(\eta\bar{\mu} - 1)}{\eta(\rho + \alpha\eta)}}, \text{ and } \beta = \sqrt{\frac{2V(0)}{\rho + \alpha\eta}}. \tag{64}$$

Remark 3: *When ρ and η are chosen as follows:*

$$\rho = \frac{2}{\lambda_m}, \ \eta = \frac{2}{\mu_m}, \tag{65}$$

the finite L_2 gains γ_1 and γ_2 become

$$\gamma_1 = \lambda_m\sqrt{\left(\frac{1}{2} + \zeta(\bar{\lambda})\right)\left(\frac{\mu_m}{\alpha\lambda_m + \mu_m}\right)}, \tag{66}$$

$$\gamma_2 = \mu_m\sqrt{\alpha\left(\frac{1}{2} + \zeta(\bar{\mu})\right)\left(\frac{\lambda_m}{\alpha\lambda_m + \mu_m}\right)}, \tag{67}$$

where the function $\zeta(\bar{x})$ is positive definite and is represented as follows:

$$\zeta(\bar{x}) = \frac{\bar{x} - x_m}{x_m}. \tag{68}$$

IV. Control Performance

The control performance is examined through numerical simulations using the two-link robot arm shown in Fig. 2. The details of the robot arm model have been described in Reference [5]. The target orbit of the arm tip is given by a circle having its origin (x_0, y_0) at (0.4 m, 0.6 m), a radius of 0.1 m, and an angular velocity of 2π rad/s. For the output saturation function $s_i(x_i)$, as shown in (17), the following sine curve is adopted:

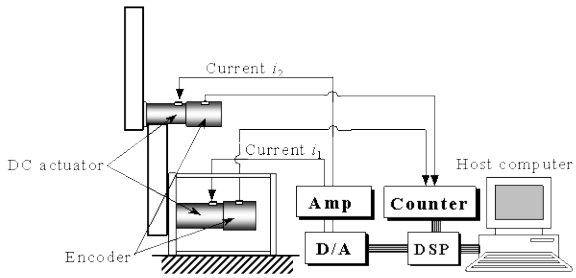

Figure 2. Schematic diagram of the robot arm model

$$s_i(x_i) = \begin{cases} 1 & \text{for} \quad \frac{\pi}{2} < x_i, \\ \sin(x_i) & \text{for} \quad -\frac{\pi}{2} \leq x_i \leq \frac{\pi}{2}, \\ -1 & \text{for} \quad x_i < -\frac{\pi}{2}. \end{cases} \tag{69}$$

Then, the value of c_i that satisfies (20) is 1/2. The following values are chosen:

$$\boldsymbol{A} = \text{diag}(50, 50), \ \boldsymbol{B} = \text{diag}(20, 20), \ \alpha = 3, \ \xi = 1, \tag{70}$$

$$\gamma_M = 6.37, \ \bar{c}_1 = \bar{c}_2 = \bar{c}_3 = \bar{c}_4 = 1, \text{ and } \bar{c}_5 = \bar{c}_6 = 7. \tag{71}$$

The input limits are assumed to be ± 6 V. The initial position is set to be $\boldsymbol{q}(\boldsymbol{0}) = [0 \quad 0]^T$, which is the straight posture stretched in the vertical direction, as shown in Fig. 2. Numerical simulations confirm that conditions (39) and (40) are satisfied for the case of no actuator saturation with the values of α, ξ, γ_M, and $\bar{c}_1 - \bar{c}_6$ given by (70) and (71).

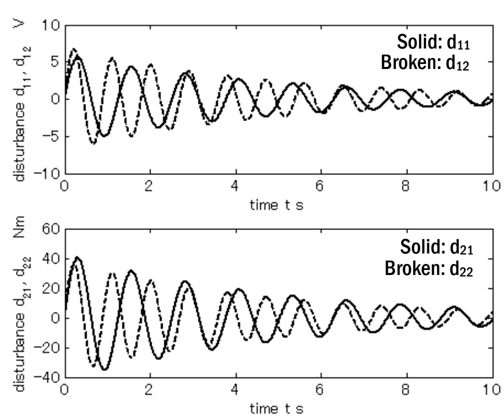

Figure 3. Examined disturbances

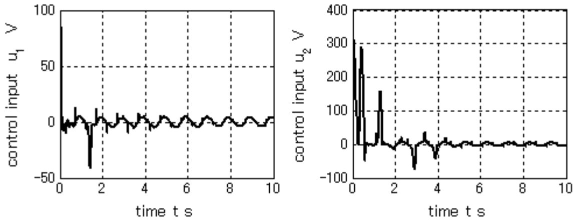

(a) Control input

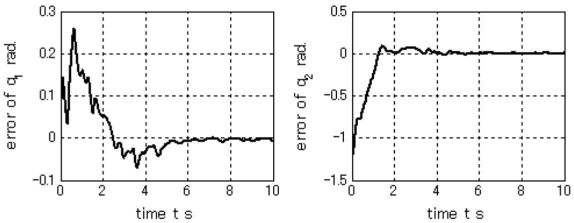

(b) Tracking error

Figure 4. Windup effect of the conventional PD adaptive control

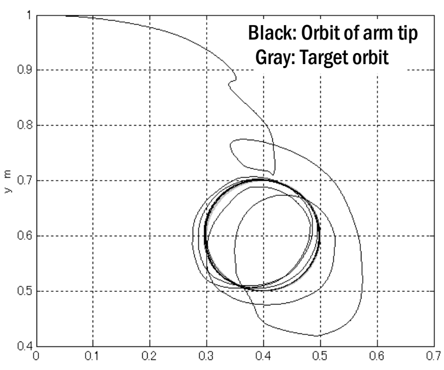

Figure 5. Arm tip orbit of the conventional adaptive PD control

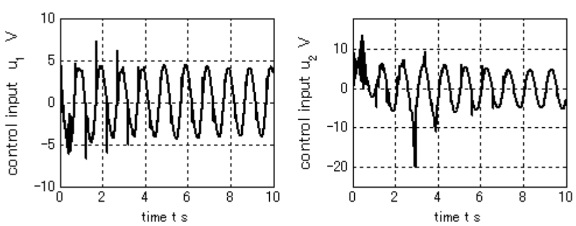

(a) Control input

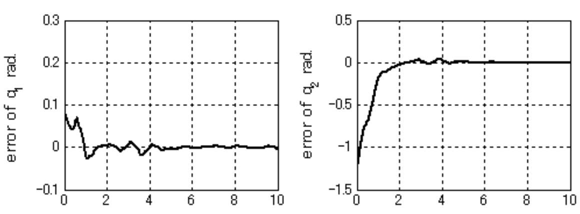

(b) Tracking error

Figure 6. Anti-windup effect of the proposed adaptive law

Fig. 3 shows the examined disturbance inputs that belong to L_2. Figs. 4 and 5 show the simulation results for the conventional PD adaptive control. As shown in Fig. 4(a), the control inputs increase significantly for the input limits ± 6 V,

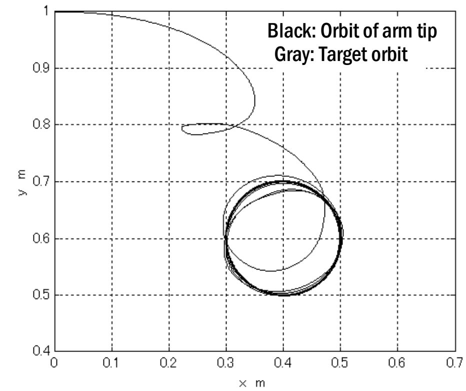

Figure 7. Arm tip orbit of the proposed anti-windup adaptive law

i.e., the windup phenomenon, so that the overshoot increases as shown in Fig. 4(b). As a result, the orbit of the arm tip degrades as shown in Fig. 5. In contrast, Figs. 6 and 7 show the simulation results using the proposed anti-windup adaptive law. As shown in Fig. 6(a), the windup effect is well restrained so that the overshoots are also restrained, as shown in Fig. 6(b), despite the disturbances. As a result, good control performance of the arm tip orbit is maintained, as shown in Fig. 7.

V. CONCLUSIONS

Local finite-gain L_2 stability using the proposed anti-windup adaptive law has been presented based on passivity for adaptive PD tracking control. The effectiveness and validity of the control method have been verified through numerical simulations using a two-link robot arm.

REFERENCES

[1] J. Zhou and C. Wen, "Robust adaptive control of uncertain nonlinear systems in the presence of input saturation," in *Proc. 14th IFAC Sympo. System Identification,* Newcastle, 2006, pp. 149–154.

[2] J. Teo and J. P. How, "Anti-windup compensation for nonlinear systems via gradient projection: Application to adaptive control," in *Proc. 48th IEEE Conf. Decision and Control and 28th Chinese Control Conf.* Shanghai, 2009, pp. 6910–6916.

[3] S. G. Khan, G. Herrmann, T. Pipe, and C. Melhuish, "Adaptive multi-dimensional compliance control of a humanoid robotic arm with anti-windup compensation," in *Proc. IEEE/RSJ International Conf. Intelligent Robots and Systems,* Taipei, 2010, pp. 2218–2223.

[4] D. J. Lopez-Araujo, A. Zavala-Rio, V. Santibanez, and F. Reyes, "Global adaptive regulation of robot manipulators with bounded inputs," in *Proc. 10th IFAC Sympo. Robot Control,* Dubrovnik, 2012, pp. 806–813.

[5] M. Kanamori, "Anti-windup adaptive law for Euler-Lagrange systems with actuator saturation," in *Proc. 10th IFAC Sympo. Robot Control,* Dubrovnik, 2012, pp. 800–805.

[6] S. Arimoto, (1996). *Control theory of non-linear mechanical systems: A passivity-based and circuit-theoretic approach,* Walton Street, Oxford OX2 6DP, New York: Oxford University Press, 1996, pp. 66–74 and 93–132.

[7] M. Kanamori, "Anti-windup adaptive tracking control for Euler-Lagrange systems with actuator saturation," in *Proc. 9th IFAC Sympo. Nonlinear Control Systems,* Toulouse, 2013, submitted for publication.

[8] M. Kanamori, "Finite-gain L_2 stability of PID set position control with anti-windup compensation for Euler-Lagrange systems with actuator saturation," in *Proc. IFAC Workshop, Lagrangian and Hamiltonian Methods for Nonlinear Control,* Bertinoro, 2012, pp. 143–148.